Available online at www.sciencedirect.com
SCIENCE DIRECT®
Journal of Organometallic Chemistry 666 (2003) 63–74
Journal of Organometallic Chemistry
www.elsevier.com/locate/jorganchem

Oxo-anion binding by metal containing molecular 'clefts'

Karl J. Wallace, Rachvinder Daari, Warwick J. Belcher, Lagili O. Abouderbala, Martyn G. Boutelle, Jonathan W. Steed *

Department of Chemistry, King's College London, Strand, London WC2R 2LS, UK

Received 1 August 2002; received in revised form 24 September 2002; accepted 25 September 2002

Dedicated to Professor Jerry L. Atwood on the occasion of his 60th birthday

Abstract

A simple but effective route has been developed to produce a series of molecular clefts, [(η^6-*p*-cymene)RuCl(**1**)$_2$]PF_6 (**4a**), [(dppe)Pd(**1**)$_2$]$(BF_4)_2$ (**5a**), [(dppe)Pd(**2**)$_2$]$(BF_4)_2$ (**5b**), [(dppe)Pt(**1**)$_2$]$(BF_4)_2$ (**6a**) and [(dppe)Pt(**2**)$_2$]$(BF_4)_2$ (**6b**), that contain either a redox active ferrocenyl or a photoactive anthracenyl side arm, attached to a ruthenium(II), palladium(II) or platinum(II) backbone. Compounds **4a**, **5a**, **5b** and **6a** act as hosts for oxo-anions. Anion recognition is achieved via convergent hydrogen bond interactions from secondary amine functionality on the side arms. The binding is also enhanced by the positive charge of the metal centres. The X-ray crystal structure of the related [$PdCl_2$(**1**)$_2$] (**7**) shows it to possess a *trans* geometry. The X-ray crystal structures of the monoadducts [(η^6-*p*-cymene)$RuCl_2$(**1**)] (**3a**) and [(η^6-*p*-cymene)$RuCl_2$(**2**)] (**3b**), which show contrasting behaviour in their hydrogen bonding to coordinated chloride, are also reported.

Keywords: Oxo-anion binding; Molecular clefts; Crystal structures

1. Introduction

Molecular recognition in host–guest complexes of anions has been of growing interest to the supramolecular chemist in recent years [1–3]. Most of these systems have used large macrocyclic *organic* building blocks such as the Calixarenes (and their derivatives) [4–6] and CTV's [7] to encapsulate the particular guest. However, the use of molecular 'tweezers' for anion recognition has been less explored in recent times [7–11]. In general, molecular tweezers, clefts or clips can be split into two categories [12]. The first are those which have flexible spacer groups and change conformation when bound to a guest [13] and secondly there are those that have a rigid spacer group, such as Kemp's triacid derivatives [14–17]. The rigid systems introduce pre-organisation in to the structure, so they can be specifically designed for a particular guest which has the correct geometry. Organic tweezers based on Kemp's triacid have been shown to bind neutral species via hydrogen bonding and π–π stacking interactions [17]. Hosts based on organic scaffolds can be very synthetically challenging although they have been extensively studied within the field of anion binding. The use of inorganic scaffolds to produce molecular clefts has been less widely explored with only a few systems being reported recently [18,19], even though these systems are frequently less synthetically problematic and exhibit versatile coordination geometries. We have recently reported a straightforward 'modular' route to a variety of anion hosts [20,21]. We now extend this simple approach to a range of molecular tweezers possessing an inorganic core coupled to either a ferrocenyl or an anthracenyl side arm.

* Corresponding author. Tel.: +44-20-78482117; fax: +44-20-78482810
E-mail address: jon.steed@kcl.ac.uk (J.W. Steed).

0022-328X/02/$ - see front matter
PII: S0022-328X(02)01962-9

2. Results and discussion

2.1. Ruthenium(II) complexes—synthesis and characterisation

Metal-containing molecular receptors that incorporate an octahedral ruthenium(II) (**4a**) or a square planar palladium(II) or platinum(II) core (**5a**,**b** and **6a**,**b**) have been prepared using a simple strategy based on ligands **1** and **2** [20]. The 3-aminopyridine-based ligands **1** and **2** were chosen because we have shown that two or three 3-aminopyridine-based units linked by a common core can produce extremely effective host compounds [20,21]. The metal centres introduce a mono or di-positive charge into the system, which contributes to anion binding. The pendant side arms **1** and **2** have a directional hydrogen bonding moieties in the form of amines, which are attached to either a ferrocenyl or anthracenyl signalling unit.

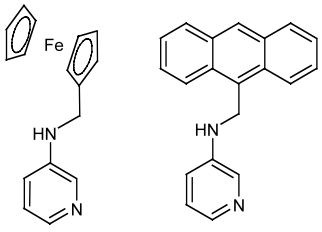

1 **2**

The ruthenium(II) receptor [(η^6-*p*-cymene)RuCl(**1**)$_2$]PF_6 (**4a**) can be synthesised either by a two-step process via the one armed adduct **3a**, or in a one-pot reaction (Scheme 1). Attempts to produce the anthracenyl species [(η^6-*p*-cymene)RuCl(**2**)$_2$]PF_6 (**4b**) by an analogous strategy were unsuccessful, apparently as a result of the steric bulk of **2**. The stepwise approach potentially has the advantage off being more versatile as the metal may be functionalised with other pyridyl groups to produce unsymmetrical, chiral hosts. Thus reaction of the intermediate adduct **3a** with one equivalent of 3-aminopyridine gives the mixed-arm complex [(η^6-*p*-cymene)RuCl(**1**)(3-aminopyridine)Cl]PF_6 (**4c**) which possesses a chiral ruthenium(II) centre. However, **4c** proved to be in equilibrium with **4b** and the analogous bis(3-aminopyridine) derivative, [(η^6-*p*-cymene)RuCl(3-aminopyridine)$_2$]PF_6 (Scheme 1). The coordination of the side arm ligands to the ruthenium(II) centre in **3a** and **4a** was confirmed by ^{1}H-NMR spectroscopy in $CHCl_3$-*d*, elemental analysis and by FAB-mass spectrometry (see Section 4). For example, the AA′BB′ resonances of the *p*-cymene protons are found at 5.36 and 5.51 ppm, respectively for the free [(*p*-cymene)$RuCl_2$]$_2$ dimer [22] but on complexation with the relevant side arm there is typically an up field shift of $\Delta\delta$ 0.16. The NH peaks appear at 6.65 ppm for the free receptor **4a** and undergo exchange on the addition of

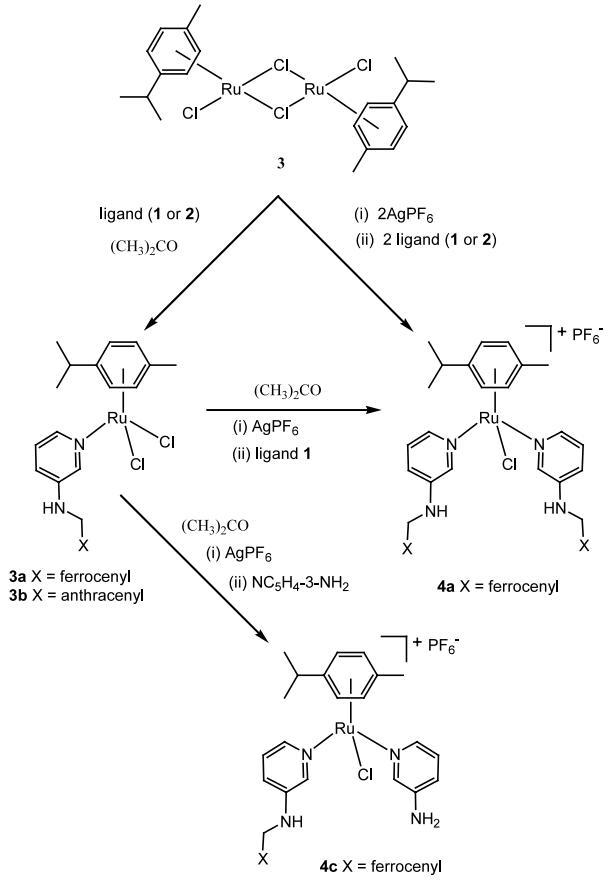

Scheme 1. Synthesis of ruthenium(II) receptors.

D_2O. The solid state infrared spectrum (Nujol mull) of **4a** displays a single ν(NH) stretch at 3414 cm^{-1}. This compares to 3313 and 3270 cm^{-1} in adducts **3a** and **3b** and 3248 and 3215 cm^{-1} in the free ligands **1** and **2**, respectively. The X-ray crystal structures of free ligands **1** and **2** show that the secondary amine is involved in NH$\cdots$pyridyl hydrogen bonding interactions [23] which represent stronger hydrogen bonds than the interactions to coordinated chloride in compounds **3a** and **3b** (vide infra), and implies that the even weaker hydrogen bonding in **4a** is to the poorly accepting PF_6^- anion.

Unlike **4a** and the analogous bis(3-aminopyridine) complex, **4c** is chiral at the ruthenium(II) centre and hence exhibits a diastereotopic ^{1}H-NMR spectrum. This is particularly evident in the *p*-cymene aryl protons which take on the form of an AA′BX pattern.

The neutral adducts **3a** and **3b** were also characterised by X-ray crystallography. Crystals were grown by slow diffusion of ether into a chloroform solution of the compounds. However, the quality of the crystals was poor and the best samples proved to be weakly diffracting and showed some evidence of twinning. As a result the overall precision is poor, however the molecular geometry and crystal connectivity are unambiguous (Fig. 1).

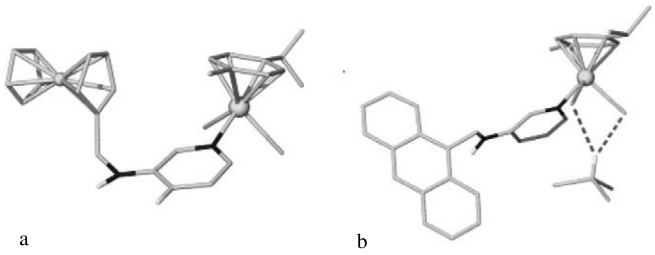

Fig. 1. View of the X-ray crystal structures of neutral molecules **3a** and **3b**. Hydrogen atoms are removed for clarity except the NH, PyH and $CHCl_3$. Selected bond lenghs (Å): **3a** Ru(1)–Cl(1) = 2.416(4), Ru(1)–Cl(2) = 2.411(4), Ru(1)–N(1) = 2.116(10); **3b** Ru(1)–Cl(1) = 2.406(11), Ru(1)–Cl(2) = 2.416(11), Ru(1)–N(1) = 2.133(3).

The crystal structure determinations of both **3a** and **3b** show the compounds to be hydrogen-bonded polymers in the solid state. However, the nature of the intermolecular interactions in the two adducts is different. The monomeric units in **3a** are connected together by the NH functionality from the amine and a CH moiety from the pyridyl ring in one molecule, hydrogen bonded to the two 'Ru–Cl' moieties from the neighbouring molecule (Fig. 2). The structure of **3b** includes an enclathrated molecule of chloroform and one of the Ru–Cl unit hydrogen bonds to the NH of the adjacent molecule and the chloroform is hydrogen-bonded to both the Ru–Cl moieties in a bifurcated fashion. This is thought to be due to the bulkiness of the anthracene groups which are unable to form the cyclic hydrogen bonded unit as seen in the ferrocene structure. The π-stacking between the anthracene units (Fig. 3), also contributes to the crystal packing (Fig. 4).

Brammer et al. have shown that directional preference for hydrogen bond donors towards terminal metal halides, in particular chloride, can be attributed to electronic effects arising from the electrostatic potential around the halide, which can be rationalised by simple orbital model of metal halide binding [24]. Generally, hydrogen bond donor groups which hydrogen-bond with a metal-chloride will interact in an orthogonal direction, therefore calculations suggest that a bifurcated hydrogen bonding arrangement is most favourable in these systems. This is indeed observed in most octahedral systems when chloride ligands are facially arranged and in square planar species of type MCl_4^{n-} ($n = 1, 2$) [25–27], but contrasts to the Ru–Cl···H–N hydrogen bond interaction in Fig. 2. This mode of interaction is relatively unusual, as it might have been predicted that the NH might have been bifurcated between the two Ru–Cl moieties, instead one of the Ru–Cl interacts with the *para* hydrogen on the pyridine ring. It is facilitated by the acidity of the pyridyl CH groups. In contrast, receptor **3b**, which does display a bifurcated interaction is comparable with other systems.

Work carried out by Orpen and Taylor and Kennard has shown [27,28] that hydrogen bonding interactions between –NH and –OH with Cl^-, C–Cl and M–Cl generally fall into three categories, weak (2.95–3.15 Å), intermediate (2.52–2.95 Å) and strong (≤ 2.52 Å) [27]. The metal-coordinated chloride ligands have been shown to be just as good hydrogen bond acceptors as anionic chloride. The hydrogen bonded polymers **3a** and **3b** fall into the strong category that has been proposed by Orpen (Table 1).

2.2. Variable temperature ^{1}H-NMR studies

Cationic metallo-receptors such as the bis(ligand) complexes **4a** and **4c** could potentially exist as two conformers, *syn* and *anti* with only the *syn* isomer appropriately pre-organized for convergent anion binding using both NH groups (Scheme 2).

Recording the ^{1}H-NMR spectrum of **4a** in acetone-d_6 between 293 and 183 K in 10 K steps revealed that at very low temperatures the spectrum becomes broad with coalescence occurring at ca. 193 K. At 183 K several sets

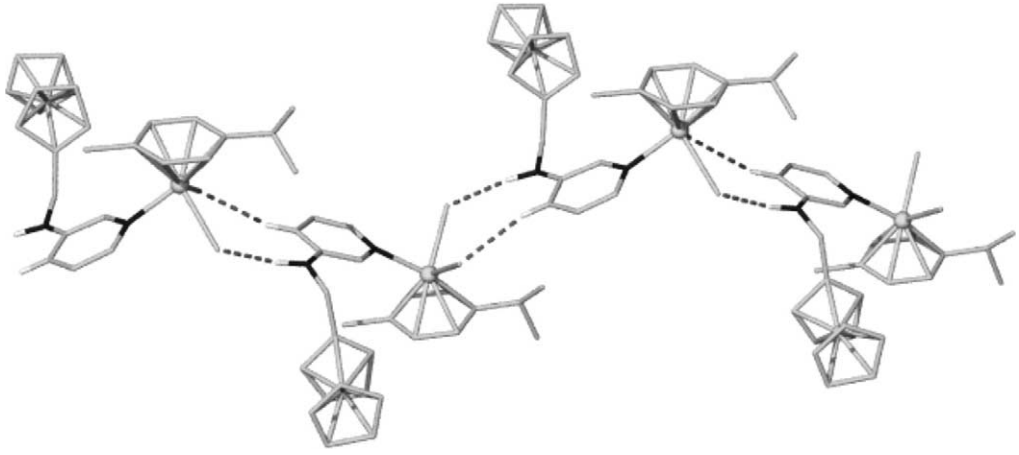

Fig. 2. Crystal packing in **3a**. Selected hydrogen bond distances (Å): N(2)–H(2N)···Cl(1), d(D···A) = 3.369(14), C(13)–H(13)···Cl(2), d(D···A) = 3.537(16).

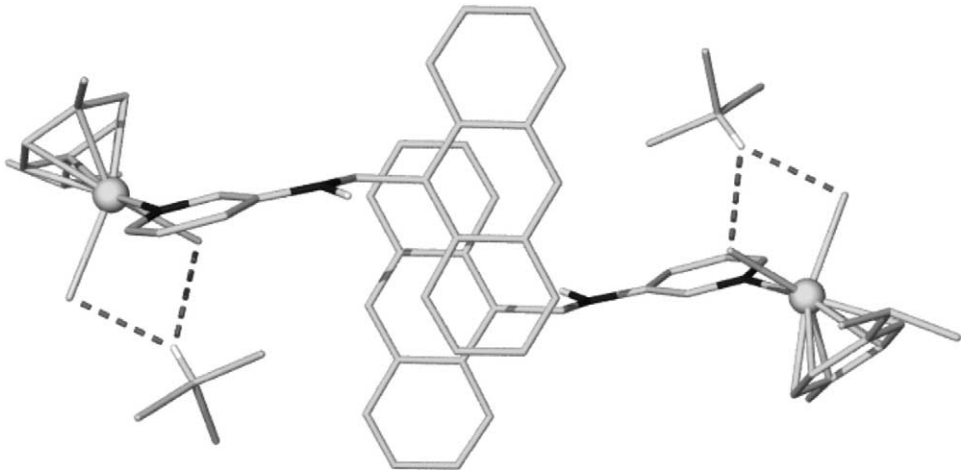

Fig. 3. π-Stacking interactions in **3b**. The distance between the anthracene rings is 3.47 Å. Selected hydrogen-bonding distances (Å): C(31)–H(31)···Cl(1), $d(D\cdots A) = 3.348(5)$, C(31)–H(31)···Cl(2), $d(D\cdots A) = 3.739(6)$.

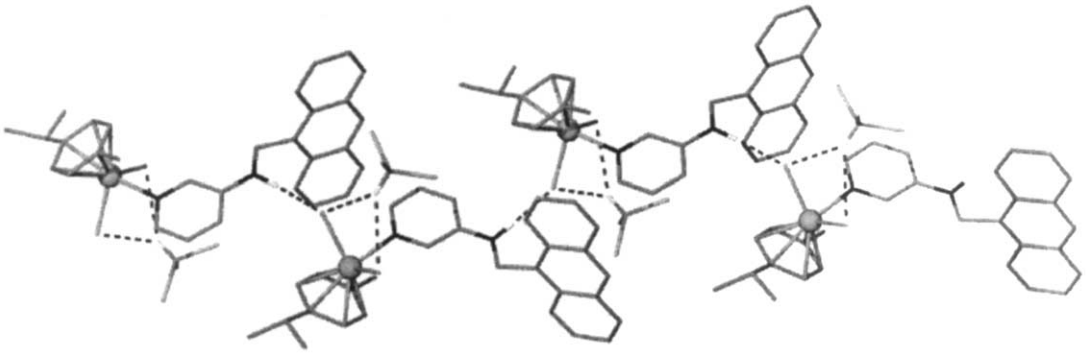

Fig. 4. Crystal packing in **3b**. Selected hydrogen bond distances (Å): N(2)–H(32)···Cl(1), $d(D\cdots H) = 0.81(5)$, $d(H\cdots A) = 2.43(5)$, $d(D\cdots A) = 3.320(4)$.

of resonances are observed assigned to the pyridyl ligands (Fig. 5a). This dynamic behaviour is attributed to the freezing out of the exchange process shown in Scheme 2. As a test of the anion binding ability of the two conformers tetrabutylammonium nitrate was added to receptor **4a** at 0.4 and 1.0 equivalents of anion and the variable temperature experiment repeated. On addition of one equivalent of $(NBu_4)NO_3$, the high temperature (293 K) spectrum shows a downfield shift of 0.37 ppm for the NH resonance to 6.55 ppm. As the sample is cooled to 183 K, the NH signal starts to split into two peaks, which suggests that there are two possible conformers. Similarly, a total of six resonances assigned to the *ortho* pyridyl CH protons are observed at 183 K shifted from their position in the hexafluorophosphate complex spectra. The fact that two resonances are approximately double the intensity of the other four suggests that the symmetrical *syn* isomer is present in approximately the same amount as the unsymmetrical *anti* form. The magnitude of the observed chemical shift changes at low temperature on addition of NO_3^- suggests that both conformations are able to interact with the anion. Interestingly, the coalescence temperature in the hexafluorophosphate experiment is ca. 10 K

Table 1
Hydrogen bonding distances (Å) in **3a** and **3b**

Compound	Interactions (Å)			
	NH···Cl	N···Cl	CH···Cl	C···Cl
3a	2.40	3.369(14)	2.62	3.37(16)
3b	2.43	3.230(4)	2.89	3.348(5)

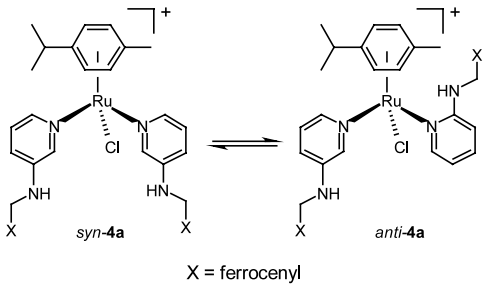

Scheme 2. Conformational exchange in **4a**.

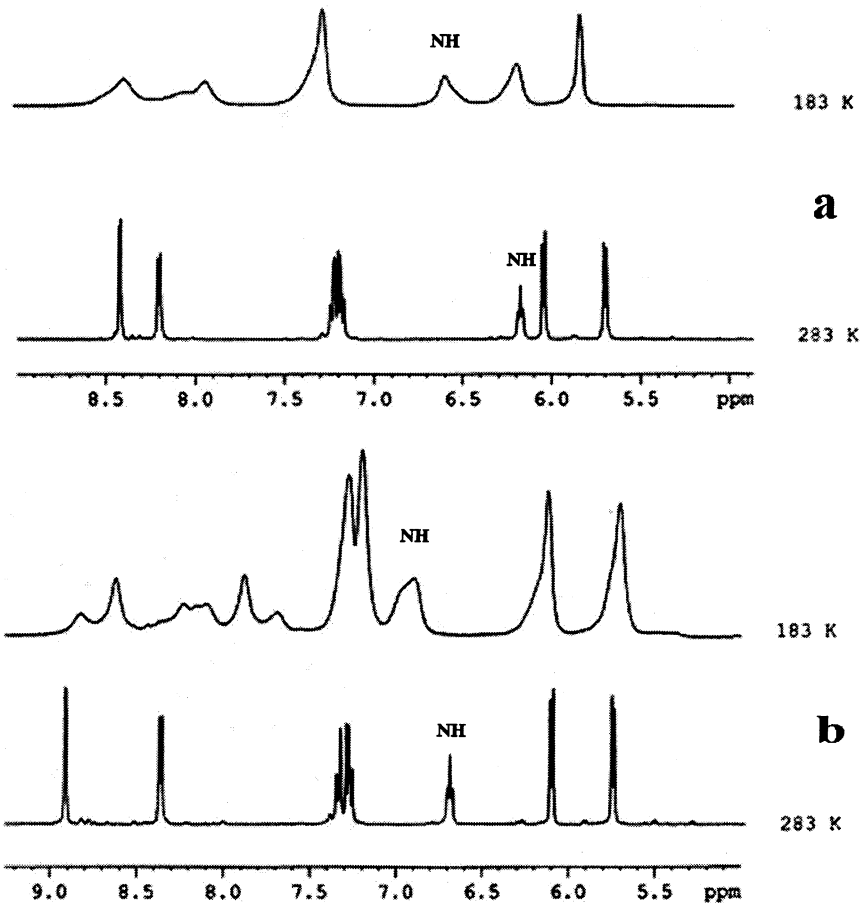

Fig. 5. Partial variable temperature (283 and 183 K) ^{1}H-NMR spectra of receptor **4a**: (a) as the hexafluorophosphate salt; and (b) after addition of one equivalent of $(NBu_4)NO_3$.

lower than after addition of NO_3^- indicating that close association with the anion retards the conformational exchange.

The fact that similar effects are seen in Fig. 5a and b (and in the 0.4 equivalent spectra) strongly suggests that the alternative explanation of the fluxional behaviour, namely slow exchange between bound and free anions is not occurring.

2.3. Palladium(II) and platinum(II) complexes—synthesis and characterisation

Attempts were made to prepare the analogous neutral *cis*-palladium(II) complex $[PdCl_2(\mathbf{1})_2]$ (**7**). A *cis* arrangement of the two pyridyl ligands is considered desirable in order to pre-organize the two NH groups for chelation of an anionic guest. The compound was prepared by refluxing $PdCl_2$ in acetonitrile, to give the $[PdCl_2(MeCN)_2]$ followed by reaction with **1**. However, X-ray diffraction studies showed that the resulting metal complex adopts a *trans* geometry (Fig. 6), as would be expected on steric grounds. The structure also incorporates a single dichloromethane molecule. The quality of the crystals were poor, however the co-ordination sphere about the palladium(II) centre and the nature of the intermolecular interactions are unambiguous (Fig. 7).

In order to enforce a *cis* geometry palladium and platinum-containing receptors were therefore synthesised, by blocking off two coordination sites of the square planar metal by reacting $[M(MeCN)_2Cl_2]$, with 1,2-bis(diphenylphosphino)ethane (dppe) to give $[M(dppe)Cl_2]^{2+}$ (M = Pd, Pt). Reaction with silver tetrafluoroborate followed by addition of two equivalents of either ligands **1** or **2** produced the desired molecular receptors $[(dppe)M(\mathbf{1})_2](BF_4)_2$ (M = Pd **5a**, Pt **5b**) and $[(dppe)M(\mathbf{2})_2](BF_4)_2$ (M = Pd **6a**, Pt **6b**) (Scheme 3).

Attempts to prepare the analogous hexafluorophosphate salts using $AgPF_6$, in acetone resulted in hydrolysis of the anion to yield $PF_2O_2^-$, clearly evident in the ^{31}P- and ^{19}F-NMR spectra. Similar problems have been reported previously [29].

The solid state IR spectra of compounds **5**, **6** and **7** each showed the expected single ν(NH) band in the range 3340–3388 cm^{-1} consistent with the NH···Cl–M interactions observed in the solid state.

The variable temperature ^{1}H-NMR spectrum of **5a** was examined in the presence and absence of

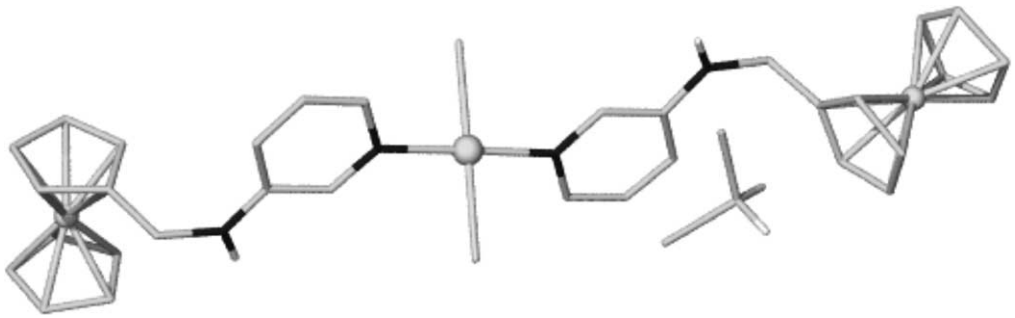

Fig. 6. X-ray crystal structure of the *trans* palladium(II) complex **7** (CH hydrogen atoms removed for clarity). Selected bond lengths (Å): Pd(1)–Cl(1) 2.297(6), Pd(1)–Cl(2) 2.308(6), Pd(1)–N(1) 2.003(17), Pd(1)–N(3) 2.038(18).

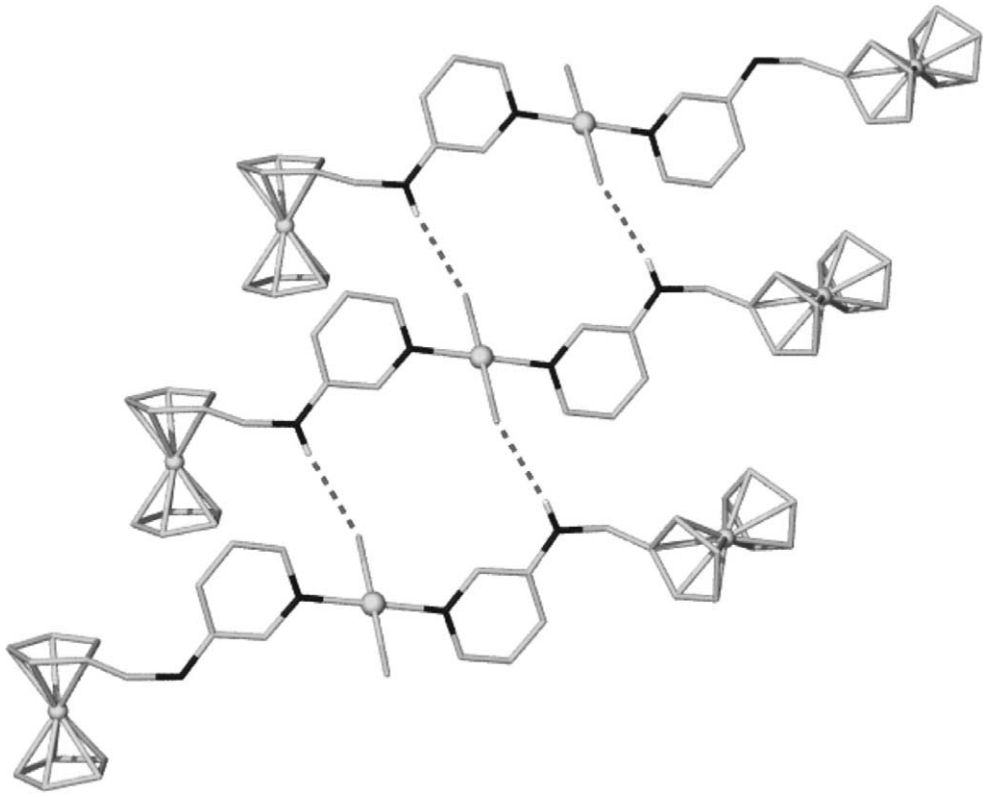

Fig. 7. Crystal packing in **7**. Selected hydrogen-bonding distances (Å): N(2)–H(2)···Cl(1), $d(D\cdots A) = 3.29(2)$, N(4)–H(4)···Cl(2), $d(D\cdots A) = 3.39(2)$.

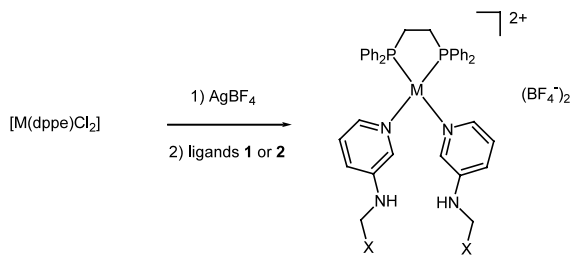

5a M = Pd, X = ferrocenyl
5b M = Pt, X = ferrocenyl
6a M = Pd, X = anthracenyl
6b M = Pt, X = anthracenyl

Scheme 3. Synthesis of palladium(II) and platinum(II) receptors.

$(NBu_4)NO_3$ as described for **4a**. Conformational exchange was not clearly observed for receptor **5a**, consistent with the less sterically hindered nature of the palladium(II) coordination environment, although some broadening occurs at 183 K. Addition of one equivalent of NO_3^- resulted in a chemical shift change of 0.25 ppm downfield for the NH resonance but no further splitting in the low temperature spectrum.

2.4. Binding studies

The anion binding behaviour of the bis(pyridyl) receptors **4a**, **5a** and **5b** was assessed by ^{1}H-NMR titration with a variety of oxo-anions in $CHCl_3$-*d*.

Limited data for the monoadduct **3a** are also included for comparison. Binding constants were calculated by least-squares non-linear fitting using the program HYPNMR [30,31] and are tabulated in Table 2. Interestingly, a good fit to the available data for **4a** was only obtained if both 1:1 and 2:1 host–anion complexes were included in the model. The importance of including species of type $(\mathbf{4a})_2X$ (X = anion) is highlighted by comparing binding curves for **4a** and **5a**, e.g. data for NO_3^- shown in Fig. 8. In the case of **4a**, most of the observed chemical shift change occurs before the addition of 0.5 equivalents of anion.

The data shown in Table 2 clearly indicate that despite the fact that both **4a** and **5a** possess the same two substituted 3-aminopyridyl ligands (**1**) arranged at ca. 90° to one another, it is the singly charged ruthenium(II) complex **4a** that is a significantly more selective host, resulting in higher effective binding constants for almost all anions studied, i.e. halides and oxoanions are bound more selectively than the competing PF_6^- and BF_4^-. This can be attributed to the lower overall positive charge on the host which decreases the non-directional electrostatic contribution to the binding, allowing greater discrimination between the target anions (particularly HSO_4^-) and the PF_6^- counter anions. Hosts based solely on electrostatic interactions tend to bind all anions equally well. Comparison with the neutral **3b** however, suggests that some positive charge is necessary and that binding is enhanced by the presence of two potentially chelating anion binding arms, consistent with previous work [20,21]. It is also possible that the poor performance of the palladium and platinum dppe systems is influenced by the bulk of the dppe ligand which may disfavour an anion chelating *syn* geometry.

The extremely high affinity for HSO_4^- may well be related to the high acidity of this anion which could result in protonation of the host secondary amine sites resulting in the formation of a ion pair between protonated host and SO_4^{2-}. Such an effect cannot be responsible for the strong binding of NO_3^-, however, and this must represent a high degree of structural complementarity between host and guest.

Table 2
Binding constants [K_{11} and K_{21} (M^{-1})] obtained for bis(pyridyl) hosts **4a**, **5a**, **5b** and **6a** [a]

	K_{11} and K_{21} (M^{-1})					
	NO_3^-	$MeCO_2^-$	ReO_4^-	$CF_3SO_3^-$	$H_2PO_4^-$	HSO_4^-
3a	17	–	–	< 10	–	–
4a	1412	[b]	~ 0	37	550	5240
	52			< 10	< 10	136
5a	15	[b]	32	26	[c]	–
5b	15	[b]	34	27	[c]	183
6a	36	–	~ 0	< 10	[c]	–

Data for the monoadduct **3a** is included for comparison.
[a] Anions added as NBu_4^+ salts. Titrations carried out in $CHCl_3$-*d* at 298 K. Errors are in the range 5–15%. K_{21} refers to the formation of species of type $(Host)_2 \cdot X$.
[b] Displacement of ligand.
[c] Precipitation.

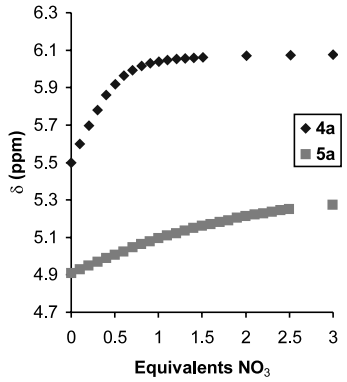

Fig. 8. ^{1}H-NMR titration curves (NH proton, $CDCl_3$, 298 K) for **4a** and **5a** with NO_3^-.

Titrations were also attempted with Cl^-, yielding K_{11} of 83 M^{-1} and K_{21} of 400 M^{-1} (two hosts to one anion) consistent with the strong halide binding observed for organic host compounds derived from **1** [20,21]. Large chemical shift changes were also observed with the pyridyl CH singlet moving 1.28 ppm and the NH resonance moving 2.44 ppm down field on addition of a total of three equivalents of chloride. However, the absolute binding constant values should be treated with caution since addition of nucleophilic anions generally proved to cause unwanted side reactions involving direct coordination to the metal centre in addition to non-covalent anion binding. Thus, over the course of a 2 h titration experiment ca. 10% of **4a** was observed to transform into the starting materials **3a** and **1**. More rapid decomposition was observed for acetate with immediate displacement of a pyridyl arm. Similar decomposition was also found on titration of **5a** and **6a** with chloride and acetate.

2.5. Electrochemical studies

The electrochemical response of the ruthenium(II) and palladium(II) receptors **4a** and **5a** as a function of added $(NBu_4)X$ concentration (X = Cl, Br, I, NO_3) was examined using cyclic voltammetry (CV). Both compounds displayed a single reversible redox couple centred on 0.552 and 0.568 V versus Ag/AgO in acetonitrile solution, respectively. This is assigned to the well known Fe(II)/Fe(III) redox couple of ferrocene. Upon titration of **4a** with up to five equivalents of Cl^- a small cathodic shift in the $E_{1/2}$ value of 17 mV was observed. Compound **5a** displayed a larger shift of 37 mV, however this is attributed to the decomplexation of

ligand **1** from the palladium(II) centre. Addition of NO_3^- and ReO_4^- to **5a** in acetonitrile gave much more modest shifts of 10 and 9 mV, respectively. Addition of NO_3^- to the ruthenium compound **4a** in acetonitrile gave a cathodic shift of 12 mV.

Changing to dichloromethane as a solvent and titrating with Cl^- resulted in a much more marked shift from 0.750 to 0.668 V, a change of some 82 mV. This is consistent with the strong binding of chloride observed in chloroform and highlights the well known effects of solvent on binding equilibria. Under the conditions of the experiment host decomposition to the parent **3a** and **1** is not extensive. The analogous titrations with Br^- and I^- produced shifts of only 25 and 10 mV, respectively, demonstrating a clear selectivity for Cl^-.

3. Conclusion

This study has shown that transition metal ions may be used as the basis of effective anion binding podands. The behaviour of the resulting inorganic hosts is influenced by the nature of the metal ion, bulk of peripheral ligands and overall complex charge, even in apparently geometrically closely related systems. This offers significant scope for fine-tuning. However, problems of host decomposition in the presence of nucleophilic anions will have to be addressed.

4. Experimental

Mass spectra were run at Kings College London on a JEOL AX505W spectrometer in fast atom bombardment (FAB) mode in a thioglycerol or nitrobenzyl alcohol matrix. NMR spectra were recorded on a Bruker AV-400 Spectrometer operating at 400 MHz. IR spectra were recorded on a Perkin–Elmer Paragon 100 Fourier transform IR spectrometer as Nujol mulls. Microanalysis was performed at the University of North London. All reactions were carried out under nitrogen, although the products showed no oxygen or moisture sensitivity. NMR titrations were carried out by using a Bruker 500 MHz spectrometer at room temperature (r.t.). All chemical shifts are reported in ppm relative to tetramethylsilane (Me_4Si).

4.1. Preparations

$[\{Ru(\eta^6\text{-}p\text{-cymene})Cl(\mu\text{-}Cl)\}_2]$, $[MCl_2(MeCN)_2]$ and $[MCl_2(dppe)]$ (M = Pd or Pt) were prepared by standard literature procedures [29,32–34].

4.2. 3-Pyridylferrocenylmethylamine (*1*)

Ferrocenecarboxaldhyde (1.00 g, 4.67 mmol) and 3-aminopyridine (0.440 g, 4.68 mmol) were dissolved in CH_2Cl_2 (50 ml) and stirred for 6 h at reflux. Sodium borohydride (1.77 g, 46.8 mmol) was added, and stirring continued for 1 h further. After this period the excess borohydride was destroyed by the dropwise addition of HCl (2 M) until effervescence was complete and the solution was slightly acidic (pH 5). Sodium hydroxide (2 M) was then added until the solution was slightly basic (pH 9). The mixture was extracted into CH_2Cl_2, washed with water, and dried over $MgSO_4$. Evaporation to dryness gave the pure product as an orange solid (1.25 g, 4.34 mmol, 93%). ^{1}H-NMR ($CHCl_3$-*d*, *J*/Hz, δ/ppm): δ 3.85 (s, br, 1H, N*H*); 3.92 (d, 2H, $J = 4.7$, CH_2); 4.08–4.12 (m, 7H, Cp*H*); 4.17 (s, 2H, CH_2); 6.85 (ddd, 1H, $J = 8.3$, 3.0, 1.4, Py*H*); 7.03 (dd, 1H, $J = 8.3$, 4.7, Py*H*); 7.92 (dd, 1H, $J = 4.7$, 1.4, Py*H*); 8.01 (d, 1H, $J = 3.0$, Py*H*). FABMS: *m*/*z* 292 $[M]^+$. IR (ν/cm^{-1}): 3248 *s* (NH). Anal. Calc. for $C_{16}H_{16}FeN_2$: C, 65.78; H, 5.52; N, 9.59. Found: C, 65.81; H, 5.45; N, 9.52%.

4.3. 3-Pyridylanthracenylmethylamine (*2*)

9-Anthracene carboxaldehyde (5.00 g, 24 mmol) and 3-aminopyridine (2.28 g, 24 mmol) were dissolved in CH_2Cl_2 (200 ml) and refluxed for 24 h under a nitrogen atmosphere. The solvent was removed under reduced pressure to produce a dark yellow oil, which was redissolved in EtOH (200 ml) and an excess of sodium borohydride (9.0 g, 240 mmol) was added to the solution and stirred at r.t. for 2 h over this time period the solution turned a light yellow. The solution was made acidic (pH 5) by the addition of 2 M HCl. This was brought back to a basic solution (pH 9) with 2 M NaOH. The product was extracted into CH_2Cl_2 (100 ml), washed several times with water (100 ml), dried over $MgSO_4$, filtered to produce a yellow solution. The solvent was removed under pressure, to produce a dark orange solid, this was chromatographed on silica gel with CH_2Cl_2–MeOH (97:3) as the eluent. The solvent was removed and re-crystallized from CH_2Cl_2 and C_6H_{14}, to yield the product as a yellow solid (3.5 g. 12.3 mmol, 51%). ^{1}H-NMR ($CHCl_3$-*d*, *J*/Hz, δ/ppm): δ 3.89 (s, br, 1H, N*H*); 5.17 (d, 2H, $J = 4.3$, CH_2); 7.11–7.13 (m, 1H, Py*H*); 7.21–7.24 (m, 1H, Py*H*); 7.50–7.59 (m, 4H, Ar*H*); 8.07 (d, 2H, $J = 8.9$, An*H*); 8.10 (m, 1H, Py*H*); 8.20 (d, 1H, $J = 2.7$, Py*H*); 8.25 (d, 2H, $J = 8.7$, An*H*); 8.52 (s, 1H, Py*H*). FABMS: *m*/*z* 284 $[M]^+$. IR (ν/cm^{-1}): 3215 *w* (NH). Anal. Calc. for $C_{20}H_{16}N_2 \cdot 2H_2O$: C, 65.78; H, 5.52; N, 9.59. Found: C, 65.81; H, 5.45; N, 9.52%.

4.4. [Ru(η⁶-p-cymene)(3-pyridylferrocenylmethylamine)Cl₂] (**3a**)

Methanol (50 ml) was degassed by bubbling nitrogen through in a 2-necked round bottom flask. [Ru(η⁶-*p*-cymene)$Cl_2]_2$ (100 mg, 0.16 mmol) and 3-pyridylferrocenylmethylamine (96 mg, 0.33 mmol) were added to methanolic solution. The solution was stirred at r.t. for 4 h, during this time period an orange solid started to form. The solid was filtered washed with MeOH and Et_2O and dried in the air for 24 h (180 mg, 92%). Orange X-ray quality crystals were obtained by $CHCl_3$–ether by slow evaporation. ^{1}H-NMR ($CHCl_3$-*d*, *J*/Hz, δ/ppm): δ 1.35 (d, 6H, $J = 6.9$, $CH(CH_3)_2$); 2.12 (s, 3H, CH_3); 3.04 (sp, 1H, $J = 6.9$, $CH(CH_3)_2$); 3.99 (d, 2H, $J = 5.3$, CH_2); (t, 2H, Cp*H*); 4.23 (s, 5H, Cp*H*); 4.29 (t, 2H, Cp*H*); 5.23, 5.46 (HAA′ HBB′, 4H, $J = 6$, Ar*H*); 6.95 (ddd, 1H, $J = 8.3$, 2.7, 1, Py*H*); 7.11 (dd, 1H, $J = 8.3$, 5.4, Py*H*); 8.35 (dd, 1H, $J = 5.4$, 1, Py*H*); 8.47 (d, 1H, $J = 2.7$, Py*H*). FABMS: *m*/*z* 598 $[M]^+$. IR (*v*/cm^{-1}): 3313 *s* (NH). Anal. Calc. for $C_{26}H_{29}Cl_2FeN_2Ru$: C, 52.28; H, 4.89; N, 4.69. Found: C, 52.04; H, 4.94; N, 9.52%.

4.5. [Ru(η⁶-p-cymene)(3-pyridylanthracenylmethylamine)]Cl₂ (**3b**)

3-Pyridylanthracenylmethylamine (539 mg, 2 mmol) and [Ru(η⁶-*p*-cymene)$Cl_2]_2$ (580 mg, 1 mmol) were dissolved in MeOH (50 ml) (previously degassed for 1 h prior to use) and stirred at r.t. for 18 h. Removal of the solvent under reduced pressure produced and orange–yellow solid that was re-crystallized from C_6H_{14}–$CHCl_3$ the solid was filtered, washed with C_6H_{14} and ether to yield the complex as a yellow solid, which was dried in the air for 24 h (480 mg, 86%). ^{1}H-NMR ($CHCl_3$-*d*, *J*/Hz, δ/ppm): δ 1.35 (d, 6H, $J = 6.9$, $(CH_3)_2$); 2.17 (s, 3H, CH_3); 3.04 (sp, 1H, $J = 7$, C*H*); 4.11 (s, br, 1H, N*H*), disappears on D_2O shake; 5.19 (d, 2H, $J = 4.3$, CH_2); 5.29, 5.45 (HAA′ HBB′, 4H, $J = 6$, Ar*H*); 7.15–7.22 (m, 2H, Py*H*); 7.53–7.62 (m, 4H, Ar*H* and Py*H*); 8.09 (d, 2H, $J = 8$, Ar*H*); 8.23 (d, 2H, $J = 8$, Ar*H*); 8.47 (d, 1H, $J = 5$, Py*H*); 8.55 (s, 1H, Py*H*); 8.62 (d, 1H, $J = 2.5$, An*H*). FABMS: *m*/*z* 590 $[M]^+$. IR (*v*/cm^{-1}): 3270 *s* (NH). Anal. Calc. for $C_{30}H_{30}Cl_2N_2Ru \cdot H_2O$: C, 57.51; H, 5.47; N, 4.47. Found: C, 57.12; H, 5.31; N, 4.42%.

4.6. [Ru(η⁶-p-cumene)(3-pyridylferrocenylmethylamine)₂Cl](PF₆) (**4a**)

[Ru(η⁶-*p*-cymene)$Cl_2]_2$ (200 mg, 0.3 mmol) and silver tetrafluorophosphate (165 mg, 0.6 mmol) were dissolved in MeOH, previously degassed for 1 h and left to stir at r.t. for 20 min, the silver(I) chloride was removed through celite and 3-pyridylferrocenylmethylamine (190 mg, 0.6 mmol) was added to the MeOH solution and stirred for a further 6 h. The solvent was removed under reduced pressure to produce a crude orange solid, which was re-crystallized from CH_2Cl_2 and C_6H_{14}. The orange solid was filtered and washed with C_6H_{14} and ether and dried in air (450 mg, 74%). ^{1}H-NMR ($CHCl_3$-*d*, *J*/Hz, δ/ppm): δ 1.13 (d, 6H, $J = 6.8$, $CH(CH_3)_2$); 1.73 (s, 3H, CH_3); 2.54 (sp, 1H, $J = 6.8$, Me_2CH); 3.98 (d, 4H, $J = 5$, CH_2); 4.10–4.28 (m, 18H, Cp*H*); 5.50 (s, br, 2H, N*H*), disappears on D_2O shake; 5.56, 5.82 (HAA′ HBB′, 4H, $J = 5.7$, Ar*H*); 6.91 (d, 2H, $J = 7.9$, Py*H*); 7.06 (t, 2H, $J = 6$, Py*H*); 8.21 (d, 2H $J = 5$, Py*H*); 8.66 (s, 2H, Py*H*). FABMS: *m*/*z* 1002 $[M+2H]^+$, 855 $[M-PF_6]^+$. IR (*v*/cm^{-1}): 3414 *w* (NH), 840 *s* (PF_6). Anal. Calc. for $C_{42}H_{46}ClF_6Fe_2N_4PRu$: C, 50.44; H, 4.64; N, 5.60. Found: C, 50.36; H, 4.69; N, 5.68%.

4.7. [Ru(η⁶-p-MeC₆H₄CHMe₂)(3-pyridylferrocenylmethylamine)(3-aminopyridine)Cl]PF₆ (**4c**)

[Ru(η⁶-*p*-cymene)(3-pyridylferrocenylmethylamine)Cl_2] (200 mg, 0.33 mmol) and silver hexafluorophosphate (85 mg, 0.33 mmol) were dissolved in MeOH (70 ml), Which was degassed prior to use, under nitrogen and stirred at r.t. for 1 h. The silver(I) chloride was filtered through celite and 3-aminopyridine (31 mg, 0.33 mmol) was added to the orange solution and stirred at r.t. for a further 6 h. The solvent was reduced to 20 ml and left to crystallize, producing a pale yellow solid which proved to be an approximately statistical mixture (2:1:1) of the desired compound, **4a** and [Ru(η⁶-*p*-cymene)(3-aminopyridine)$_2$Cl]PF_6. ^{1}H-NMR ($CHCl_3$-*d*, *J*/Hz, δ/ppm): δ 1.07 (d, 6H, $J_{obs} = 7.0$, $CH(CH_3)_2$); 1.67 (s, 3H, CH_3); 2.47 (sp, 1H, $J = 7.0$, C*H*); 3.92 (d, 2H, $J = 5.2$, CH_2); 4.03–4.21 (m, 9H, Cp*H*); 4.95 (t, H, $J = 5.2$, N*H*); 5.41 (d, 1H, $J = 5.5$, Ar*H*); 5.50 (d, 1H, $J = 5.5$, Ar*H*); 5.73 (d, 2H, $J = 5.5$, Ar*H*); 6.80–7.00 (m, 2H, Py*H*); 8.23 (m, 2H, Py*H*); 8.60 (s, 1H, Py*H*); 8.63 (s, 1H, Py*H*). FABMS: *m*/*z* 655 $[M-PF_6]^+$. IR (*v*/cm^{-1}): 3414 *w* (NH), 3342 *w* (NH), 3227 *w* (NH), 850 *s* (PF_6). Anal. Calc. for $C_{31}H_{36}ClF_6FeN_4PRu$: C, 46.43; H, 4.52; N, 6.99. Found: C, 46.41; H, 4.43; N, 6.94%.

4.8. [Pd(dppe) bis(3-pyridylferrocenylmethylamine)](BF₄)₂ (**5a**)

[$PdCl_2$(dppe)] (115 mg, 0.22 mmol) and $AgBF_4$ (96 mg, 0.44 mmol) was dissolved in a previously degassed solution of C_3H_6O (100 ml) and left to stir for 30 min. The white AgCl ppt was filtered through celite and 3-pyridylferrocenylmethylamine (131 mg, 0.44 mmol) was added to the C_3H_6O solution and left to stir at r.t. for 4 h. The solvent was then reduced to half its volume and Et_2O was added to yield a yellow solid, which was filtered and washed with ether and dried in air for 24 h (258 mg, 93%). ^{1}H-NMR ($CHCl_3$-*d*, *J*/Hz, δ/ppm): δ

2.81 (m, 2H, CH_2); 2.86 (m, 2H, CH_2); 3.61 (s, 4H, CH_2); 4.11–4.18 (m, 18H, CpH); 4.91 (s, br, 2H, NH), disappears on D_2O shake; 6.54 (d, 2H, $J=8$, PyH); 6.758 (t, 2H, $J=7.6$, PyH); 7.32–7.63 (m, 20H, ArH); 7.71 (d, 2H $J=4$, PyH); 8.36 (s, 2H, PyH). $^{31}P\{^1H\}$-NMR ($CHCl_3$-d): δ 64 (s). FABMS: 1086 m/z $[M-2BF_4]^+$. IR (ν/cm^{-1}): 3387 w (NH), 1049 s (BF_4). Anal. Calc. for $C_{58}H_{56}B_2F_8Fe_2N_4P_2Pd$: C, 55.17; H, 4.47; N, 4.44. Found: C, 55.24; H, 4.39; N, 4.38%.

4.9. [Pt(dppe)(3-pyridylferrocenylmethylamine)$_2$](BF$_4$)$_2$ (**5b**)

[$PtCl_2$(dppe)] (100 mg, 0.15 mmol) and $AgBF_4$ (59 mg, 0.3 mmol) was dissolved in a previously degassed solution of C_3H_6O (100 ml) and left to stir for 30 min. The white silver(I) chloride ppt was filtered through celite and 3-pyridylferrocenylmethylamine (88 mg, 0.3 mmol) was added to the C_3H_6O solution and left to stir at r.t. for 4 h. The solvent was removed under reduced pressure to produce the crude yellow Pt complex which was re-crystallized from cyclohexane, to produce the desired complex as a yellow solid (170 mg, 84%). ^{1}H-NMR ($CHCl_3$-d, J/Hz, δ/ppm): δ 2.62 (m, 2H, CH_2); 2.66 (m, 2H, CH_2); 3.71 (d, 4H, $J=5$, CH_2); 4.03–4.10 (m, 18H, CpH); 5.16 (s, br, 2H, NH), disappears on D_2O shake; 6.53 (d, 2H, $J=8$, PyH); 6.82 (t, 2H, $J=7.6$, PyH); 7.48–7.52 (m, 12H, ArH); 7.65–7.72 (m, 10H, ArH and PyH); 8.11 (s, 2H, PyH). $^{31}P\{^1H\}$NMR ($CHCl_3$-d): δ 37 (t, $+J_{Pt-P}=3209$). FABMS: m/z 1175 $[M-2BF_4]^+$. IR (ν/cm^{-1}): 3388 w (NH), 1047 s (BF_4). Anal. Calc. for $C_{58}H_{56}B_2F_8Fe_2N_4P_2Pt$: C, 51.55; H, 4.18; N, 4.15. Found: C, 51.59; H, 4.16; N, 4.08%.

4.10. [Pd(dppe) bis(3-pyridylanthracenylmethylamine)](BF$_4$)$_2$ (**6a**)

[$PdCl_2$(dppe)] (400 mg, 0.7 mmol) and silver tetrafluroroborate (271 mg, 1.4 mmol) were dissolved in C_3H_6O (100 ml), previously degassed for 1 h, and stirred at r.t. for 20 min. The silver(I) chloride was removed through celite and 3-pyridylanthracenylmethylamine (396 mg, 1.4 mmol) was added to the C_3H_6O solution and stirred for 18 h. The solvent was concentrated to 15 ml under reduced pressure and left to crystallize. The creamy white solid was filtered and washed with ether to yield the desired product as an air stable compound (723 mg, 83%). ^{1}H-NMR (MeCN-d_3, J/Hz, δ/ppm): δ 2.90 (m, 2H, CH_2); 2.97 (m, 2H, CH_2); 4.90 (d, 4H, $J=4$, CH_3); 5.02 (s, br, 2H, NH), disappears on D_2O shake; 7.15 (s, 4H, PyH); 7.53 (m, 8H, PyH and AnH); 7.66 (m, 9H, AnH and ArH); 7.73 (m, 11H, AnH and ArH and PyH); 7.82 (m, 4H, PyH); 8.10 (m, 8H, AnH+PyH); 8.61 (s, 2H, AnH). $^{31}P\{^1H\}$NMR (MeCN-d_3): δ 66 (s). FABMS: m/z 1073 $[M-2BF_4]^+$. IR (ν/cm^{-1}): 3398 w (NH), 1011 s (BF_4). Anal. Calc. for $C_{66}H_{56}B_2F_8N_4P_2Pd$: C, 63.60; H, 4.53; N, 4.49. Found: C, 63.62; H, 4.86; N, 4.34%.

4.11. [Pt(dppe)(3-pyridylanthracenylmethylamine)$_2$](BF$_4$)$_2$ (**6b**)

[$PtCl_2$(dppe)] (200 mg, 0.3 mmol) and silver tetrafluoroborate (117 mg, 0.6 mmol) were dissolved in C_3H_6O 100 ml, which was previously degassed and allowed to stir at r.t. for 20 min. The silver(I) chloride was removed by filtering through celite and 3-pyridylanthracenylmethylamine (171 mg, 0.6 mmol) was added to the solution, which was refluxed for 6 h. The solvent was concentrated to 15 ml and allowed to crystallize. The white solid that was formed was filtered and washed with ether and dried in air for 24 h (206 mg, 52%). ^{1}H-NMR (MeCN-d_3, J/Hz, δ/ppm): δ 3.62 (m, 4H, CH_2); 4.87 (d, 4H, $J=4$, CH_2); 5.02 (br, s, 2H, NH), disappears on D_2O shake; 7.14 (m, 4H, PyH); 7.53–7.93 (m, 32H, AnH and ArH and PyH); 7.98 (m, 4H, PyH); 8.15 (m, 4H, PyH); 8.63 (s, 2H, AnH). $^{31}P\{^1H\}$-NMR (MeCN-d_3): δ 45 (t, $J_{Pt-P}=2794$). FABMS: m/z 1162 $[M-BF_4]^+$. IR (ν/cm^{-1}): 3400 w (NH), 1001 s (BF_4). Anal. Calc. for $C_{66}H_{56}B_2F_4N_4P_2Pt$: C, 59.34; H, 4.23; N, 4.19. Found: C, 59.37; H, 4.41; N, 4.25%.

4.12. trans-[Pd(3-pyridylferrocenylmethylamine)$_2$Cl$_2$] (7)

[$PdCl_2$(MeCN)$_2$] (200 mg, 0.77 mmol) and 3-pyridylferrocenylmethylamine (453 mg, 1.5 mmol) were dissolved in CH_2Cl_2, previously degassed and stirred at r.t. for 4 h. The solvent was removed under reduced pressure and the crude orange solid was re-crystallized from CH_2Cl_2 and Et_2O, the yellow–orange solid was filtered washed with ether and dried in air (500 mg, 85%). ^{1}H-NMR (DMSO-d_6, J/Hz, δ/ppm): δ 4.01 (d, 4H, $J=5.3$, CH_2); 4.12 (s, 4H, CpH); 4.22 (s, 10H, CpH); 4.29 (s, 4H, CpH); 6.54 (t, 2H, $J=5$, PyH); 7.13 (s, 4H, PyH and NH); 7.84 (dd, 2H, $J=1.4$, 4, PyH); 8.13 (s, 2H, PyH). FABMS: m/z 761 $[M]^+$. IR (ν/cm^{-1}): 3352 w (NH). Anal. Calc. for $C_{32}H_{32}Cl_2Fe_2N_4Pd$: C, 50.46; H, 4.23; N, 7.36. Found: C, 50.38; H, 4.14; N, 7.26%.

4.13. X-ray crystallography

Crystals were mounted using silicon grease on a thin glass fibre. All crystallographic measurements were carried out with a Nonius KappaCCD diffractometer equipped with graphite monochromated Mo–K_α radiation using wide ϕ and ω scans. Data collection temperature was 120 K, maintained by using an Oxford Cryosystem low temperature device. Diffractometer control and data collection strategy used the COLLECT package [35]. Indexing, integration and scaling were

carried out by the DENZO-SMN package [36]. Data sets were corrected for Lp effects and for the effects of absorption (Scalepack) and crystal decay where appropriate. Structures were solved using the direct methods option of SHELXS-97 [37] and developed using conventional alternating cycles of least-squares refinement (SHELXL-97 [38]) and difference Fourier synthesis with the aid of the program XSEED, which was also used to prepare the diagrams [39]. In all cases non-hydrogen atoms were refined anisotropically except for some disordered, while C–H hydrogen atoms were fixed in idealized positions and allowed to ride on the atom to which they were attached. Hydrogen atom thermal parameters were tied to those of the atom to which they were attached. Where possible acidic hydrogen atoms were located experimentally and their positional and displacement parameters refined. All calculations were carried out on an IBM-PC compatible personal computer.

4.13.1. Crystal data for **3a**

$C_{26}H_{30}Cl_2FeN_2Ru$, $M = 598.34$, orange needles, $0.10 \times 0.02 \times 0.02$ mm^3, orthorhombic, space group $P2_12_12_1$ (No. 19), $a = 11.7739(11)$, $b = 12.7969(10)$, $c = 16.1921(12)$ Å, $V = 2439.7(3)$ Å^3, $Z = 4$, $D_{calc} = 1.629$ g cm^{-3}, $F(000) = 1216$, 12 760 reflections collected, 4276 unique ($R_{int} = 0.1640$). Final goodness-of-fit = 1.247, $R_1 = 0.1019$, $wR_2 = 0.1676$, R indices based on 3408 reflections with $I > 2\sigma(I)$ (refinement on F^2), 287 parameters, 36 restraints. Lp and absorption corrections applied, $\mu = 1.450$ mm^{-1}. The best crystals available proved to be small, weakly diffracting and showed evidence of twinning. The absolute parameter of 0.56(10) suggests racemic twinning, which was modeled accordingly.

4.13.2. Crystal data for **3b**

$C_{31}H_{31}Cl_5N_2Ru$, $M = 709.90$, yellow block, $0.40 \times 0.30 \times 0.20$ mm^3, monoclinic, space group $P2_1/n$ (No. 14), $a = 12.668(3)$, $b = 17.210(3)$, $c = 13.981(3)$ Å, $\beta = 94.764(3)^\circ$, $V = 3037.6(10)$ Å^3, $Z = 4$, $D_{calc} = 1.552$ g cm^{-3}, $F(000) = 1440$, 9535 reflections collected, 4046 unique ($R_{int} = 0.0335$). Final goodness-of-fit = 1.018, $R_1 = 0.0385$, $wR_2 = 0.0888$, R indices based on 3590 reflections with $I > 2\sigma(I)$ (refinement on F^2), 369 parameters, 0 restraints. Lp and absorption corrections applied, $\mu = 0.980$ mm^{-1}.

4.13.3. Crystal data for **7**

$C_{33}H_{34}Cl_4Fe_2N_4Pd$, $M = 846.54$, orange blocks, $0.20 \times 0.15 \times 0.10$ mm^3, monoclinic, space group $P2_1/c$ (No. 14), $a = 16.4874(15)$, $b = 7.444(3)$, $c = 27.574(6)$ Å, $\beta = 106.327(4)^\circ$, $V = 3247.7(15)$ Å^3, $Z = 4$, $D_{calc} = 1.731$ g cm^{-3}, $F(000) = 1704$, 12 994 reflections collected, 5455 unique ($R_{int} = 0.1340$). Final goodness-of-fit = 1.090, $R_1 = 0.1596$, $wR_2 = 0.3475$, R indices based on 3340 reflections with $I > 2\sigma(I)$ (refinement on F^2), 398 parameters, 12 restraints. Lp and absorption corrections applied, $\mu = 1.790$ mm^{-1}. The best crystals available proved to be small, weakly diffracting and showed evidence of twinning.

4.14. ^{1}H-NMR titrations

NMR titrations were carried out by using a Bruker 500 MHz spectrometer at r.t. All chemical shifts are reported in ppm relative to Me_4Si. A specific concentration, typically 0.05 M, of the host was made up in a single NMR tube in the desired deuterated solvent (0.5 ml). The anions, as the tetrabutylammonium $[(Bu)_4N^+X^-]$ salts were made up in a 2 ml volumetric flask, five times the concentration of the host, with the desired deuterated solvent. Ten microlitre aliquots of the guest were then added to the NMR tube and the spectra were recorded after each addition.

4.15. Electrochemistry

Electrochemical experiments were performed in a low volume three-electrode cell in dry, degassed MeCN, analyte concentration 5×10^{-4} M. The background electrolyte was NBu_4PF_6 (0.1 M). The working electrode was a Pt disc of 2 mm diameter and the auxiliary a Pt wire. Potentials are reported relative to Ag/AgO in background electrolyte against which ferrocene is oxidised at 0.512 V. To prevent fouling the working electrode was polished before each addition of anion. Cyclic voltammetry and differential pulse voltammetry was performed using Chart 1.5.2 (ADInstruments) running on a Powerlab 4 s/p (ADInstruments). The potentiostat was a Biosensor II potentiostat (EMS Ltd.).

5. Supplementary material

Crystallographic data for the structural analysis have been deposited with the Cambridge Crystallographic Data Centre, CCDC Nos. 191220–191222 for compounds **3a**, **3b** and **7**. Copies of this information may be obtained free of charge from The Director, CCDC, 12 Union Road, Cambridge CB2 1EZ, UK [Fax: (int code) +44-1223-336033; e-mail: deposit@ccdc.cam.ac.uk or www: http://www.ccdc.cam.ac.uk).

Acknowledgements

We thank the EPSRC and King's College London for funding of the diffractometer system and Dr L.J. Barbour for the program X-SEED used in the X-ray structure determinations.

References

[1] M.M.G. Antonisse, D.N. Reinhoudt, Chem. Commun. (1998) 443.
[2] J.L. Atwood, J.W. Steed, Structural and topological aspects of anion coordination, in: K. Bowman-James, A. Bianchi, E. Garcia-Espana (Eds.), Supramolecular Chemistry of Anions, Wiley-VCH, Weinheim, 1997, pp. 171–177.
[3] P.A. Gale, Coord. Chem. Rev. 199 (2000) 181.
[4] P.D. Beer, M.G.B. Drew, K. Gradwell, J. Chem. Soc. Perkin Trans. 2 (2000) 511.
[5] Y.H. Shi, H.J. Schneider, J. Chem. Soc. Perkin Trans. 2 (1999) 1797.
[6] M. Staffilani, K.S.B. Hancock, J.W. Steed, K.T. Holman, J.L. Atwood, R.K. Juneja, R.S. Burkhalter, J. Am. Chem. Soc. 119 (1997) 6324.
[7] K.T. Holman, M.M. Halihan, S.S. Jurisson, J.L. Atwood, R.S. Burkhalter, A.R. Mitchell, J.W. Steed, J. Am. Chem. Soc. 118 (1996) 9567.
[8] M.J. Gunter, M.R. Johnston, B.W. Skelton, A.H. White, J. Chem. Soc. Perkin Trans. 1 (1994) 1009.
[9] M. Harmata, C.L. Barns, S.R. Karra, S. Elahmad, J. Am. Chem. Soc. 116 (1994) 8392.
[10] S. Yaghi, H. Kitayama, T. Takagishi, J. Chem. Soc. Perkin Trans. 1 (2000) 925.
[11] P.D. Beer, Acc. Chem. Res. 31 (1998) 71.
[12] J.W. Steed, K.J. Wallace, Podand hosts for anion binding and signalling, in: G.W. Gokel (Ed.), Advances in Supramolecular Chemistry, vol. 9, JAI Press, London, 2002, in press.
[13] R. Sylvie, L.B. Metz, A.A. Varneck, M. Gross, New J. Chem. 21 (2000) 371.
[14] J. Rebek, Jr., B. Askew, M. Killoran, D. Nemeth, F.T. Lin, J. Am. Chem. Soc. 109 (1987) 2426.
[15] D.S. Kemp, K.S. Peteakis, J. Org. Chem. 46 (1981) 514.
[16] G. Smith, U.D. Wermuth, J.M. White, Chem. Commun. (2000) 2349.
[17] J. Rebek, Jr., K.D. Shimizu, T.M. Dewey, J. Am. Chem. Soc. 116 (1994) 5149.
[18] C.R. Bondy, P.A. Gale, S.J. Loeb, Chem. Commun. (2001) 729.
[19] P.D. Beer, Acc. Chem. Res. 31 (1998) 71.
[20] L.O. Abouderbala, W.J. Belcher, M.G. Boutelle, P.J. Cragg, J.W. Steed, D.R. Turner, K.J. Wallace, Proc. Natl. Acad. Sci. USA 99 (2002) 5001.
[21] L.O. Abouderbala, W.J. Belcher, M.G. Boutelle, P.J. Cragg, M. Fabre, J. Dhaliwal, J.W. Steed, D.R. Turner, K.J. Wallace, Chem. Commun. (2002) 358.
[22] M.A. Bennett, A.K. Smith, J. Chem. Soc. Dalton Trans. (1974) 233.
[23] K.J. Wallace, J.W. Steed, (2002) unpublished results.
[24] L. Brammer, E.A. Bruton, P. Sherwood, Cryst. Growth Des. 1 (2001) 277.
[25] L. Brammer, J.K. Swearingen, E.A. Bruton, P. Sherwood, Proc. Natl. Acad. Sci. USA 99 (2002) 4956.
[26] M. Calleja, S.A. Mason, P.D. Prince, J.W. Steed, C. Wilkinson, New J. Chem. 25 (2001) 1475.
[27] G. Aullón, D. Bellamy, L. Brammer, E.A. Burto, A.G. Orpen, Chem. Commun. (1998) 653.
[28] (a) G.A. Jeffrey, An Introduction to Hydrogen Bonding, OUP, Oxford, 1997 79–97.;
(b) R. Taylor, O. Kennard, J. Am. Chem. Soc., 104 (1982) 5063–5070.
[29] M.A. Bennett, A.K. Smith, J. Organomet. Chem. 175 (1979) 87.
[30] P. Gans, HypNMR 2000, University of Leeds, Leeds, 2000.
[31] C. Frassineti, S. Ghelli, P. Gans, A. Sabatini, M.S. Moruzzi, A. Vacca, Anal. Biochem. 231 (1995) 374.
[32] J.R. Doyle, P.E. Slade, H.B. Jonassen, Inorg. Synth. 6 (1960) 213.
[33] J.M. Jenkins, J.G. Verkade, Inorg. Synth. 11 (1968) 108.
[34] W.L. Steffen, G.J. Palenik, Inorg. Chem. 15 (1976) 2432.
[35] R. Hooft, COLLECT, Nonius B.V., Delft, 1998.
[36] Z. Otwinowski, W. Minor, Methods in enzymology, in: C.W. Carter, R.M. Sweet (Eds.), Methods in Enzymology, vol. 276, Academic Press, London, 1997, pp. 307–326.
[37] G.M. Sheldrick, SHELXS-97, University of Göttingen, 1997.
[38] G.M. Sheldrick, SHELXL-97, University of Göttingen, 1997.
[39] L.J. Barbour, XSeed, University of Missouri, Columbia, 1999.